JOURNAL OF NEUROTRAUMA
Volume 19, Number 10, 2002

Axonal Injury in Children after Motor Vehicle Crashes: Extent, Distribution, and Size of Axonal Swellings Using β-APP Immunohistochemistry

CATHERINE GORRIE,[1] SAMANTHA OAKES,[1] JOHAN DUFLOU,[2] PETER BLUMBERGS,[3] and PHIL M.E. WAITE[1]

ABSTRACT

The brains of 32 children (3 months to 16 years) who died as a result of motor vehicle collisions were examined for axonal injury using β-APP immunohistochemistry. The extent and distribution of axonal injury was assessed and quantified throughout the forebrain, brainstem and cerebellum. The mean diameter of immunoreactive axons in the corpus callosum was measured for this pediatric group and, for comparison, a small adult sample. β-APP immunoreactivity was seen in 14 pediatric cases (survival 35 mins to 87 h), most frequently in the parasagittal white matter (12/14), the corpus callosum (11/14), the brainstem (10/14) and cerebellum (9/14). In 2 cases, axon swelling was visualized in the internal capsule after only 35–45-min survival, earlier than has previously been reported. No immunoreactivity was seen in the remaining 18 cases who died within 1 h. The extent and distribution of axonal injury throughout the brain showed a rapid early increase with increasing survival time and then a slower progression. The diameter of individual callosal axons increased with increasing survival times, rapidly over the first 24 h and then more slowly. There was no statistical difference ($p < 0.05$) for callosal axon diameters at different survival times between the children and the adults sampled here. The extent and distribution of axonal injury throughout the brain appears to be similar in children to that previously reported in adults. The spatial and temporal spread of axonal damage suggests there may be therapeutic potential for the process to be arrested or slowed in its early stages.

Key words: β-APP; axon diameter; axonal injury

INTRODUCTION

WIDESPREAD DAMAGE TO AXONS in the white matter of the brain (diffuse axonal injury; DAI) is a well-recognized consequence of traumatic head injury (reviewed in Adams et al., 1991; Graham et al., 2000). DAI has been shown to be present in head injury caused by motor vehicle accidents (MVAs) (Blumbergs et al., 1989), falls (Abou-Hamden et al., 1997), assaults (Graham et al., 1992) and gunshot wounds (Koszyca et al., 1998). Patients who sustain severe DAI are typically unconscious from the moment of impact, do not experience a lucid period and remain vegetative or at least severely disabled until death (Blumbergs et al., 1989). Diagnosis

[1]Neural Injury Research Unit, School of Medical Sciences, University of New South Wales, Sydney, Australia.
[2]Department of Forensic Medicine, Sydney Central Area Health Service, Sydney, Australia.
[3]Neuropathology Laboratory, Institute of Medical and Veterinary Science, Adelaide, Australia.

of DAI is usually made in these patients following investigation by CT scans or MRI and in the absence of a large expanding intracranial hematoma. Post mortem diagnosis may be aided by the presence of a number of "hallmark" lesions, specifically, focal hemorrhage in the corpus callosum, or in the dorsolateral quadrant of the rostral brainstem and gliding contusions in the parasagittal white matter (Adams et al., 1982, 1986). A definitive diagnosis can only be made at autopsy by the visualization of axonal injury such as swollen axons or axonal bulbs.

Motor vehicle accidents are a common cause of nonmissile head injury in humans and usually involve a high acceleration/deceleration force as well as a rotational component. Animal models in nonhuman primates (Gennarelli et al., 1982; Maxwell et al., 1993) and pigs (Meaney et al., 1995; Smith et al., 1997) have shown both of these factors to be important in producing axonal injury.

It is becoming widely accepted that DAI is the result of a secondary process of traumatic head injury (Fitzpatrick et al., 1998) especially in the lower range of injury severity. Primary axotomy may occur at the time of injury in severe head trauma, but recent work has provided a consensus that axons can undergo a sequence of change following an initial insult that culminate in a so-called secondary axotomy over a period of time (Maxwell et al., 1997). The specific cellular mechanisms of axonal swelling and disconnection are still unknown and a number of different hypotheses are under investigation (Adams, et al., 1989; Waxman et al., 1993; Povlishock, 1992; Maxwell et al., 1997). The current pathogenesis of this traumatic injury is that focal, intra-axonal disruption of the cytoskeleton occurs which leads to impaired axonal transport causing gradual axonal swelling as products accumulate at the site. Disconnection can occur many hours or even days later as the axon finally breaks (Povlishock and Jenkins, 1995). β-Amyloid precursor protein (β-APP) is a membrane spanning glyco-protein of nerve cells which is transported by fast axoplasmic flow, and is one such product that accumulates following cytoskeletal disruption (Koo et al., 1990). β-APP immunohistochemistry has been shown to be an effective marker for this process (Gentleman et al., 1993; Sherriff et al., 1994). Theoretically this process could be arrested or slowed, making its time course in humans of relevance.

While traumatic axonal injury has been well documented in adults, relatively few studies have investigated the distribution or time course in children. Differences might be expected in view of the different properties of the skull and reduced myelination of the pediatric brain (Brody et al., 1987). Graham et al. (1989) found that many types of brain damage identified in children were remarkably similar to those seen in adults. The main difference was that children tended to show more brain swelling than their adult counterparts. However, the distribution and time course of axonal injury as identified by β-APP immunohistochemistry was not examined in this sample.

Our current study examined the brains of child road fatalities with the intent of assessing the extent and distribution of axonal injury in relation to survival time. Our aim was to determine whether microscopic features of axonal injury in children vary from that reported for adults.

MATERIALS AND METHODS

The sample used in this study consisted of a total of 32 children under the age of 16 years who died as a result of a motor traffic accident in the Sydney metropolitan area and cases under 5 years in rural NSW. The post mortem findings of the body and brain injuries and the neurovascular damage in this sample has been reported previously (Gorrie et al., 2001). A subset of this sample showing axonal injury was examined in detail, in the present study, for the distribution of injury throughout the brain and for the diameter of injured axons in the corpus callosum.

All these cases were subject to full post mortem examination at the Dept. of Forensic Medicine as required under the NSW Coroners Act. The multidisciplinary approach used to study the events associated with each fatality has been explained previously (Gorrie et al., 1999). For the neurological assessment, brains were immersion fixed in 10% formalin for a minimum of 2 weeks. Prior to dissection the brains were photographed in the ventral, dorsal and lateral views. The brainstem and cerebellum were then removed and three fiducial markers (to aid in the later reconstruction of sections) were inserted through the cerebrum in the horizontal plane. The cerebrum was sliced in the coronal plane at a thickness of 10 mm. The first cut was made through the mammillary bodies and slices were labeled A1 up to A6 anteriorly, and P1 up to P6 posteriorly. Four parasagittal sections were taken through each half of the cerebellum and the brainstem was sliced into 8–10 transverse sections through the pons and medulla. All slices were photographed and embedded in paraffin wax before sections were taken at a thickness of 8–10 μm. Two sections underwent routine staining for hematoxylin and eosin (H&E) to visualize general morphology and Luxol fast blue (LFB) to differentiate white matter tracts. A third section was immunoreacted with a mouse monoclonal antibody against β-APP (Boehringer Mannheim diluted 1:50) and incubated

overnight at 4°C. Sections were then incubated in a biotinylated secondary antibody against mouse IgG (Sigma) diluted 1:200 for 1 h and were visualized by the ABC method using nickel enhanced DAB as the chromogen. For negative controls, primary antibody was omitted.

Axonal Injury Distribution and Extent

To assess the extent of axonal damage, all β-APP–stained sections were examined at 100 times magnification and all areas showing axonal damage were marked with a Nikon object marker (0.05 cm^2) attached to the microscope. These marked sections were then digitally scanned, and using NIH image analysis software (NIH, 1996), were aligned and overlaid with a sector grid (Blumbergs et al., 1995; Koszyca et al., 1998). Each brain was then scored using two different methods:

1. An axonal injury sector score (AISS) was derived for each brain by counting the number of sectors (Fig. 1A,B) showing injury divided by the number of sectors examined. This score was adjusted for all cases to give a score out of 116, the maximum possible number of sectors in a brain.
2. The area of injury was measured for each coronal section using NIH image with the method described by Gorrie et al. (1999). The proportion of injury in each section was determined and recorded as a percentage of the total area for the whole brain. Individual areas such as the corpus callosum (sector 1) and parasagittal white matter (sectors 7 and 8) could then be assessed separately in the same manner.

Injury Distribution Within the Corpus Callosum

For all brains showing axonal injury in the corpus callosum ($n = 11$), the percentage of axonal injury was measured in each section containing the corpus callosum (sector 1). Brain sections A1 and P1 were at the level of the mammillary bodies and therefore represented the body of

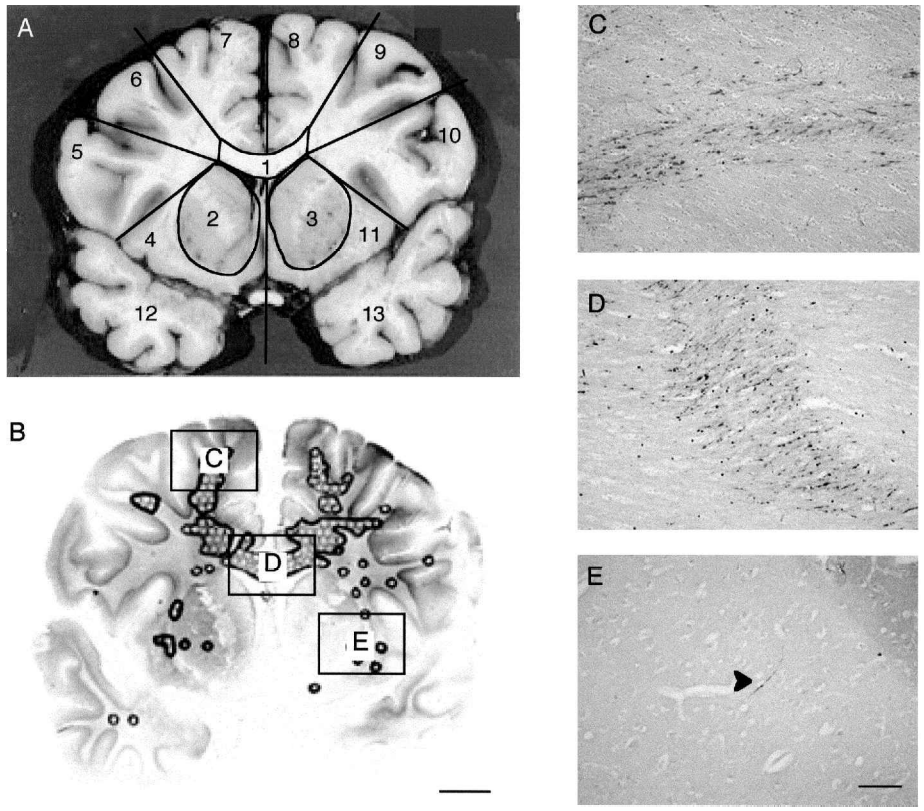

FIG. 1. (**A**) Coronal section A1 from case 8 (7-h survival) with an overlaid sector grid dividing the section into 13 sectors. (**B**) The corresponding β-APP–stained section showing the distribution of injured axons (marked areas). The β-APP staining in this case is predominantly located in the corpus calosum and the parasagittal white matter. Examples of the appearance of these axons are shown in boxes C, D, and E. (**C**) Clusters of injured axons running parallel to the fibre tract in the parasagittal white matter. (**D**) Bands of injured axons within the corpus callosum. (**E**) Single isolated immunopositive axon (arrowhead). Bars = 1 cm (A,B), 100 μm (C,D).

the corpus callosum. The anterior sections contained the genu, and the posterior sections contained the splenium of the corpus callosum. The sections showing the greatest amount of axonal damage in the corpus callosum were then determined for each brain.

Corpus Callosal Axon Diameter

β-APP–stained sections through the body of the corpus callosum were examined in detail in a subset of 11 pediatric cases from this study sample. Additionally, sections from a further three child cases and 12 adult cases of known survival time were obtained for analysis (courtesy of P. Blumbergs, Adelaide). These additional pediatric cases were included to provide a wider range of survival times and the adult cases were necessary for direct comparison of axon diameters. All the corpus callosal sections were immunoreacted and analysed by the same person using identical methods.

For each case, approximately 100 β-APP–positive axons were randomly sampled. A horizontal line approximately 2 cm in length was marked on the coverslip on each section of the corpus callosum. The first 100 immunopositive axons adjacent to that line were collected as digital images at $\times$400 magnification. As swollen axons are irregular in appearance, Euclidian distance mapping (Russ, 1994) was used to determine and measure the widest diameter of the axon profile using a program developed for NIH image software. The mean and standard error of the axon diameters for each case was then calculated. A two-tailed *t* test was used to compare the coefficient and constant for the lines of best fit for the pediatric and adult samples.

RESULTS

Pediatric Sample

Thirty-two cases of child road fatalities considered here included pedestrians, vehicle passengers, and one cyclist. Axonal injury was seen in 14 of these cases (Table 1) in which the survival times ranged from 0.6 to 87 h. The remaining 18 cases died at the accident scene or shortly after, none had survival times greater than one hour, and none had any evidence of axonal damage as visualized by β-APP immunohistochemistry, so are not considered further. All 14 cases with positive immunoreactivity displayed evidence of head impact although the actual cause of death was not necessarily attributable to head injury alone. Ten patients were admitted to hospital, all were unconscious and died without recovering consciousness. Four cases underwent CT or MRI scans and showed evidence of skull fractures, shearing injuries, increased ICP and/or cerebral oedema. Surgical intervention was undertaken in two cases to relieve pressure due to brain swelling. Hemorrhagic shock was noted in two cases and four patients were maintained on artificial life support for a period of several hours. The time of death was taken to be the time of clinical brain death for these patients (Table 1). Hypoxic changes were noted in these four cases and in two additional cases with longer survival times (27 and 87 h).

Morphology of Damaged Axons

Damaged axons presented as strongly β-APP positive against a pale background. They showed one or more of the following morphologies: continuous enlarged longi-

Table 1. Details of the Study Sample of 14 Children with Diffuse Axonal Injury after Motor Vehicle Crashes

Case	*Age (y)*	*Sex*	*Survival time (h)*	*Type*	*Cause of death*
1	0.25	F	0.58	Passenger	Head injury
2	2	M	0.75	Pedestrian	Multiple injuries
3	14	M	1	Pedestrian	Multiple injuries
4	12	M	1	Passenger	Head injury
5	11	F	2	Passenger	Multiple injuries
6	15	F	2.3	Passenger	Multiple injuries
7	4	M	5[a] (19)	Pedestrian	Multiple injuries
8	8	M	7	Pedestrian	Multiple injuries
9	12	M	7.5[a] (23)	Cyclist	Head injury
10	5	F	8	Pedestrian	Multiple injuries
11	16	F	12[a] (22)	Pedestrian	Head injury
12	8.5	M	27	Pedestrian	Head injury
13	2	F	52[a] (91)	Passenger	Head injury
14	8	F	87	Pedestrian	Head injury

[a]Time until clinical brain death. Time until cessation of life support system shown in brackets.

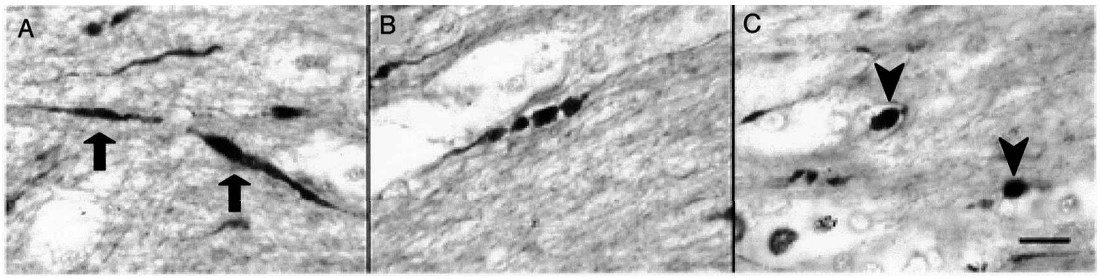

FIG. 2. Photomicrographs showing common morphologies of β-APP–positive axons in the corpus callosum in children. (**A**) Swollen profiles (arrows) in longitudinal section. (**B**) Beaded profiles. (**C**) Terminal balls or end bulbs (arrowheads). Bar = 10 μm.

tudinal profiles, discontinuous beaded profiles or terminal bulbs (Fig. 2A–C). Injured axons occurred singly or in clusters or sheets running either horizontally within a fibre tract or in bands across it (Fig. 1C–E).

Axonal Injury Distribution and Extent

For each of the 14 β-APP–positive cases, the brain was divided into a total of 116 sectors including the brainstem and cerebellum (Blumbergs et al., 1995) and positive staining was seen in 2–109 sectors. The percentage of the brain showing axonal injury ranged from 0.1% to 65%. Generally, damaged axons were distributed diffusely through the white matter of the brain although in some cases there were several distinct foci of axonal injury. Regions consistently displaying damaged axons in most of the brains were the parasagittal white matter (12/14), the corpus callosum (11/14), the brainstem (10/14), and the cerebellum (9/14), but there was no single region that was positive in all of the cases. A pale diffuse β-APP immunoreactivity was also seen in the cytoplasm of neurons throughout the cortex and central grey matter in most cases.

Correlation of axonal injury with other lesions is shown in Figure 3. Hemorrhagic lesions were found in all 14 cases and consisted of subarachnoid hemorrhage (12), small cortical lesions (8), subdural hemorrhage (5), gliding contusions (5), lesions in the corpus callosum (4), and large intracranial hematomas (2). There was no macroscopic evidence of hemorrhagic lesions in the

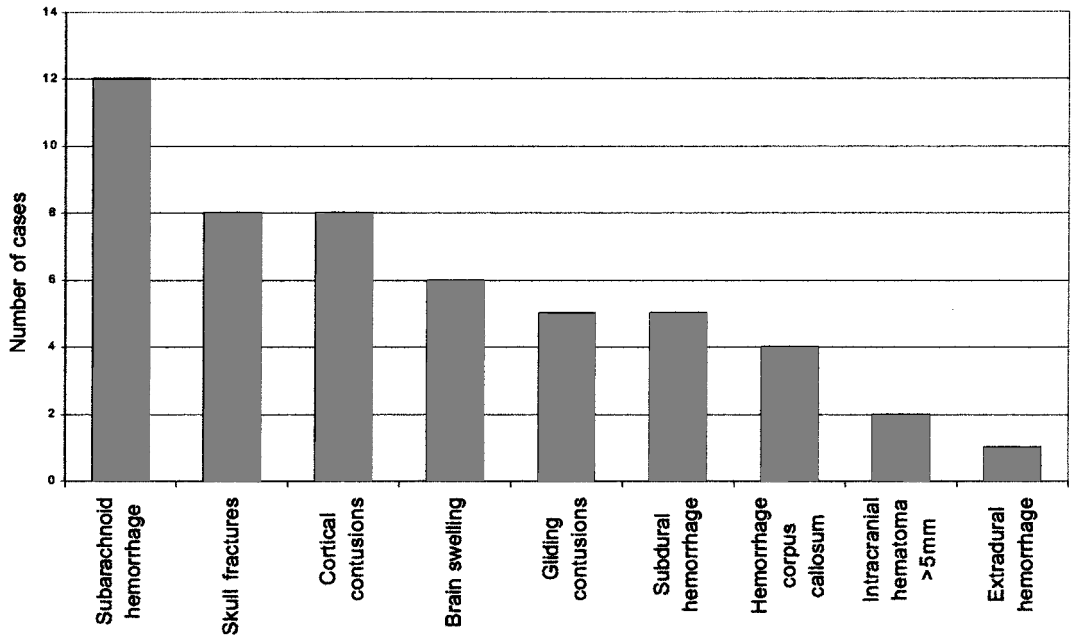

FIG. 3. Histogram showing the frequency of types of head injury and neuropathology coexisting with diffuse axonal injury in this sample of 14 pediatric cases.

dorso-lateral quadrant of the rostral brainstem in any of these cases. Eight of these children (57%) had skull fractures, and six (43%) showed signs of brain swelling. β-APP immunoreactivity was not restricted to areas immediately adjacent to sites of hemorrhage and did not appear to be closely associated with any single focal destructive lesion.

Time Course of Axonal Injury

The earliest time we were able to discern irrefutable evidence of axonal injury was at 35 min in a 3-month-old child who died as a result of a high-speed car crash; times for both the crash and death were well documented. In this case, injured axons were located in small numbers in the internal capsule, the thalamus and the brainstem (pontocerebellar tracts and medial lemniscus). Another case (a 2-year-old male) was β-APP immunopositive at 45-min survival, again with injured axons localized to the internal capsule. The axonal injury sector score (AISS) in both these cases was low and the percentage of the white matter showing injury was less than 2%.

Both the axonal injury sector score, AISS (Fig. 4A) and the percentage of injury (Fig. 4B) increased with longer survival times. The AISS values initially increased rapidly to reach 96/116 at 12 h and then rose more gradually to 108/116 by 87 h. Similarly, for the percentage area of white matter damaged, there was an initial rapid increase (33% by 12 h) followed by a slower rise to 65% by 87 h. Structures showing the highest percent of damage (Table 2) were the corpus callosum (mean 37%, maximum 87%) followed by the parasagittal white matter (mean 23%, maximum 42%), the brainstem (mean 7%, maximum 29%) and cerebellum (mean 3%, maximum 16%).

Corpus Callosal Axon Diameter

The maximum diameter of damaged axons in the corpus callosum was measured at different survival times for 14 pediatric cases and 12 adults. Diameters of β-APP–positive axons ranged from 0.43 to 13.36 μm, and diameters increased with longer survival times. Representative examples are shown in Figure 5. The mean diameter of β-APP positive axons, measured from the corpus callosum at different survival times, is shown in Figure 6. Comparison of pediatric and adult curves (Fig. 6) showed there was no significant difference, us-

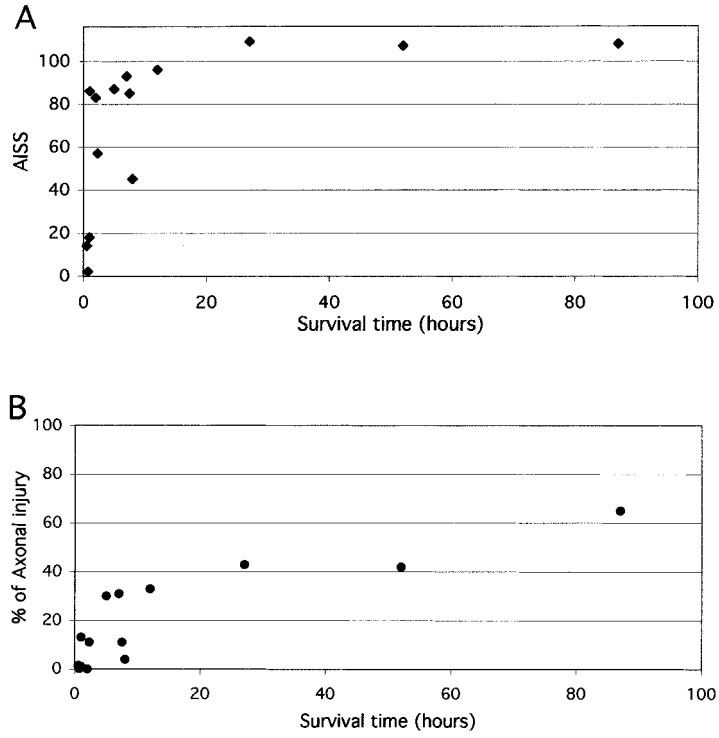

FIG. 4. Increase in the distribution of diffuse axonal injury with increasing survival times as demonstrated by Axonal Injury Sector Score (AISS) (**A**) and the percentage of axonal injury (**B**) in 14 children following motor vehicle crashes.

Table 2. The Number of Cases Showing Axonal Injury in Different Brain Regions and the Mean ± SE and Maximum Percentage of Injury Detected in the White Matter in Each of These Regions

Brain region	*No. of cases (n = 14)*	*Percentage of brain region showing injury (mean ± SE)*	*Maximum percentage of injury within brain region*
Corpus callosum	11	37.2 ± 9.0	87
Parasagittal WM	12	23.1 ± 5.4	42
Brainstem	10	6.9 ± 2.6	29
Cerebellum	9	3.3 ± 1.2	16

WM, white matter.

ing the two-tailed t test, between the coefficient ($t = 0.18$, $df = 10$, $p < 0.05$) and the constant ($t = 0.43$, $df = 10$, $p < 0.05$) for the lines of best fit generated from the two sets of data.

Injury Distribution Within the Corpus Callosum

Eleven cases showed evidence of axonal injury in the corpus callosum. The majority of the cases had 6 sections containing the corpus callosum from A3 to P3. The amount of axonal injury within all the corpus callosal sectors ranged from 10% to 100%. Figure 7 shows a histogram of the distribution of maximal axonal injury within the corpus callosum. Six cases showed the greatest amount of axonal injury in section P2 which corresponds to the posterior part of the body of the corpus callosum. Fewer cases had the maximal injury in A1(2), P1(3), and P3(1). In one case, injury was equally high in two sections (P1 and P2). No brain had maximal injury within the genu.

DISCUSSION

This paper describes the distribution and time course of axonal injury in children following road trauma, using β-APP as the marker for injury. Our main conclusions are that axonal injury in pediatric cases shows a similar morphology and location to that previously reported in adults. We show that axonal injury increases in amount and extent with increasing survival time, initially rapidly and then with a slower progression. We demonstrate that the diameter of injured axons also increases with survival duration for the first week. Finally we show that this increase in diameter has a similar time course in this pediatric sample to that from an adult sample, processed and analysed with the same methodology.

Onset of β-APP Positivity

β-APP immunohistochemistry has been shown to be the most effective method for visualizing axonal injury, being more sensitive than silver techniques (Blumbergs, 1998) or other immunohistochemical methods (Sherriff et al., 1994). In addition, it is able to detect damaged axons well before other methods (Gentleman et al., 1993; McKenzie et al., 1996; Sherriff et al., 1994). In our sample, using β-APP immunohistochemistry, we were able to demonstrate irrefutable evidence of swollen axons after 35-min and 45-min survival in two cases where the times of injury and death were known precisely. Previous studies have confirmed β-APP–positive axons as

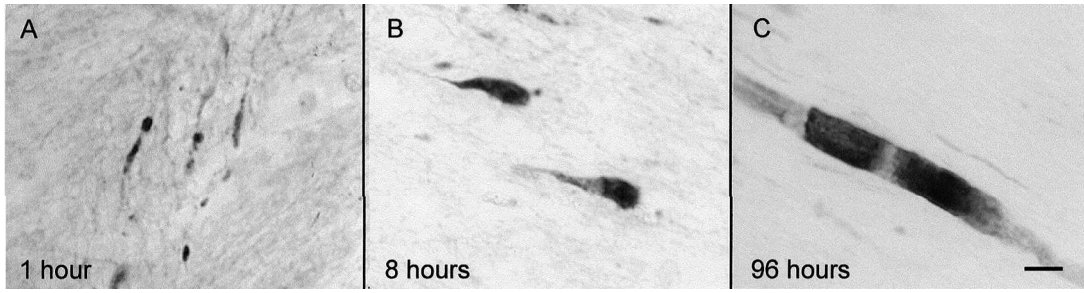

FIG. 5. β-APP–positive axons imaged from different cases with varying survival times of 1 h, (**A**) 8 h (**B**), and 96 h (**C**). They are representative of the largest axons seen in each case. Bar = 10 μm.

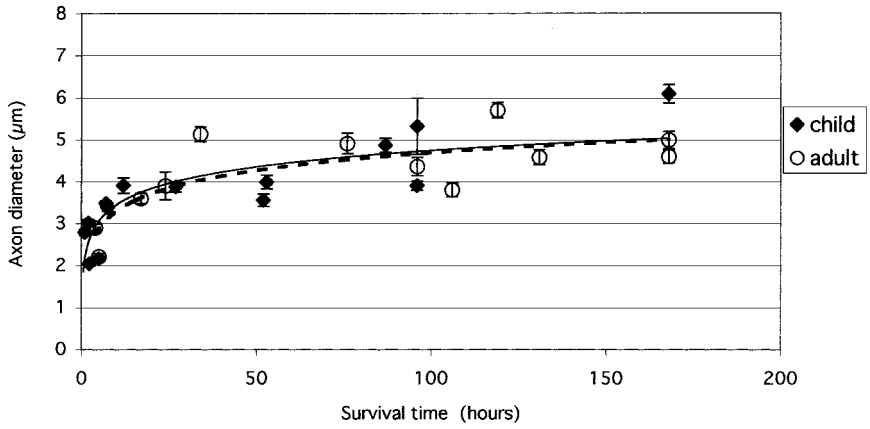

FIG. 6. Axon diameter (mean ± SE) of β-APP–positive axons in the body of the corpus callosum from 14 pediatric and 12 adult cases at different survival times. There was no significant difference between these lines of best fit ($p > 0.05$).

early as 1 h after injury in both sheep (Lewis et al., 1996) and humans (Wilkinson et al., 1999). It should be noted that the axons visualized at these earliest survival times were small and few in number, and they were localized in the internal caspule. The earlier onset seen here may be due to the immaturity of axons in these cases (3 months and 2 years). From animal studies, the rates of fast anterograde axonal transport are known to be faster in young axons (Politis and Ingoglia, 1979; Viancour and Kretier, 1993). Alternatively, this early onset may represent an especially vulnerable region of the pediatric brain for axonal injury. A recent study of head inflicted injury in very young children (2–3 months) has identified another region of axonal vulnerability located at the craniocervical junction (Geddes et al., 2001).

Morphology and Distribution of Injured Axons

The neuropathological appearance of injured axons in children appears to be similar to that previously described in adults (Abou-Hamden et al., 1997; Koszyca et al., 1998), with axonal enlargement, beading, and spheroids all seen here. The arrangement of small clusters of damaged axons as well as the bands of β-APP–positive fibers seen in these children's brains have been described in adult brain samples (Gentleman et al., 1993; McKenzie et al., 1996, Abou-Hamden et al., 1997). Also, low lev-

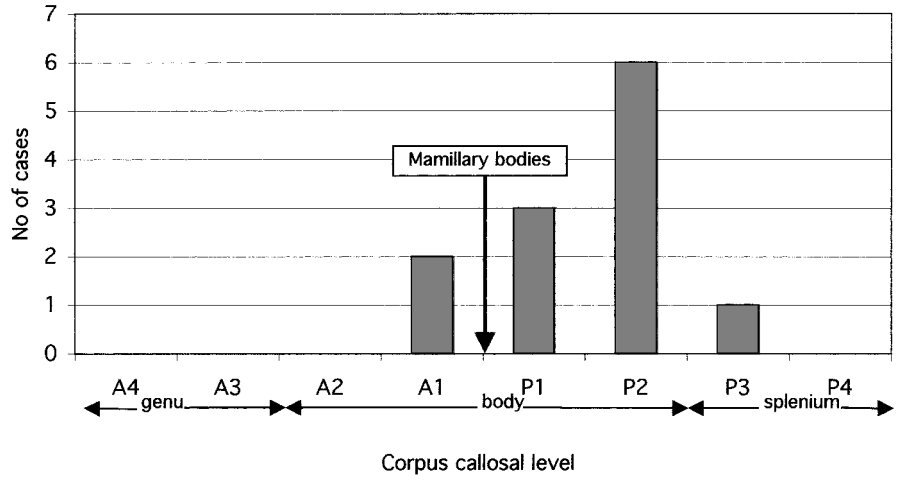

FIG. 7. Histogram showing the distribution of the maximal axonal injury throughout the corpus callosum in 11 pediatric brains. A4 to P4 are the anterior-posterior sections of the brain containing the corpus callosum. One case had an equally high amount of axonal injury in two levels P1 and P2.

els of staining in cortical neurons and central/internal gray matter have been previously noted (Gentleman et al., 1993).

The areas most commonly showing injury in our pediatric sample, the parasagittal white matter and corpus callosum, are similar to the areas most frequently showing injury after trauma in adults (Adams et al., 1989). Similarly, no unusual distribution of injury was noted in the three pediatric cases (8, 14, and 16 years) included in the study by Blumbergs et al. (1995). Using the same sector scoring method to study injury distribution following falls in adults, Abou-Hamden et al. (1997) showed axonal injury was present in the central grey matter and corpus callosum in all cases and was common in the brainstem (94%) and cerebral hemispheric white matter (94%). This is similar, though somewhat higher than the present results for corpus callosum (11/14, 78%), brainstem (10/14, 71%), and cerebral hemispheric white matter (12/14, 86%). A study using a standardized impact injury in lambs also showed the same distribution of injury patterns as in adult sheep (Finnie et al., 1999). Therefore it would appear that the cellular mechanisms of this type of injury are independent of age. Similarly the maturation of the developing skull and brain is not a contributing factor in determining the distribution of axonal injury, although it is known to affect the extent of vascular injury and skull fracture (Slazinski and Johnson, 1994; Templeton, 1993). Both skull fractures and SAH are higher in this pediatric sample with DAI (fractures, 57%; SAH, 86%) than reported in adults (skull fractures, 29%, Adams et al., 1982; SAH, 62%; 5/8 adult cases Gultekin and Smith, 1994). Despite the expectation that deformation may be greater in the softer immature skull and therefore shearing within the brain would be larger, the present results indicate a similar extent and distribution of axonal injury regardless of age. Finnie et al., (1999) suggest that the greater deformation of the immature brain is partly mitigated by greater compliance of the young skull allowing for more absorption of the impact force.

Progression of Injury Distribution

The two pediatric cases showing injury at less than 1 h both had a few damaged axons localized in the deep cerebral white matter of the internal capsule. With longer survival times the number and distribution of damaged axons became more extensive. Both the number of sectors showing axonal injury, and the percentage area of injury in the entire brain, reflect this rise. By 30 h post incident, nearly all the sectors (100/116) were showing evidence of swollen axons and, in the longest surviving case, axonal injury eventually involved over half of the total white matter. Similarly, axonal injury sector scores of 91–110/116 were reported in adults with severe closed head injury after long survival times (Blumbergs et al., 1995). A confounding variable in relation to survival time is impact force, which was unable to be standardized in this study. In four cases where the head impact force had been previously calculated (Gorrie et al., 2001), no obvious pattern of axonal injury distribution was associated with increased impact force. Similarly, biomechanical data, such as the height of a fall was not found to be a predictor of the extent and severity of axonal injury in 16 adults (Abou-Hamden et al., 1997).

In medicolegal cases, establishing the time of death and whether it is related to traumatic injury can be crucial and Geddes et al. (2000) have discussed the possibility of using β-APP staining for establishing both the time of death and its association with trauma. However, it is now well recognized that β-APP staining is not specific for traumatic damage. Axonal injury secondary to hypoxia/ischemia is common and has a similar appearance (Blumbergs, 1998). Moveover, the distribution of traumatic and hypoxic injury can be difficult to distinguish, particularly at short survival times (Geddes et al., 2000). Both traumatic and hypoxic axonal injury are likely to share a similar pathogenesis, with a change in membrane permeability leading to Ca^{2+} entry, activation of proteases and disruption of the cytoskeleton (Povlishock et al., 1995; Maxwell et al., 1997; Blumbergs, 1998). Although the present study and others (McKenzie et al., 1996; Oehmichen et al., 1998) have shown an increase in the amount and distribution of β-APP immunopositivity with increasing survival, our data would indicate that this was too variable to be useful in the timing of the trauma.

Injury Distribution Within the Corpus Callosum

A particularly clear example of the similarity of axonal injury distribution in the pediatric and adult brain is shown for the corpus callosum. Our study indicates a peak of injury within the corpus callosum in section P2, at the mid-thalamic level. This is identical to the site of maximal callosal injury in a recent study of eight adult males (17–83 years), also using β-APP immunohistochemistry (Leclercq et al., 2001). Similarly MRI findings indicate that the posterior corpus callosum suffers the greatest traumatic injury in adults (Gentry et al., 1988) and children (Mendelsohn et al., 1992). Traumatic lesions in the corpus callosum are consistent with shear stress patterns within the brain and internal partitions (Nishimoto et al., 1998). Gentry et al. (1988) suggest that the selective vulnerability of the posterior corpus callosum may be due to the fact that the falx is wider posteriorly and prevents displacement of the brain across the midline to the same extent as anteriorly. This causes greater shear and tensile strains to develop in the posterior part of the corpus callosum compared to the genu where some

of the shear strain is shared by the brain tissue. For axonal injury, it may be relevant that this posterior region contains the largest diameter axons within the corpus callosum (Aboitiz et al., 1992). This could confer increased vulnerability, or it may make visualization with β-APP immunohistochemistry more obvious.

Corpus Callosal Axon Diameter

Data from axon diameters rather than distribution of damage may be of more value for establishing the time of trauma (Fig. 6). Oehmichen et al. (1998) described β-APP as a marker of vitality meaning that, as a forensic tool, it is useful in determining a period of survival. Increase in diameter of β-APP–positive axon profiles requires continuing axonal transport to the injury site thus allowing transported proteins, β-APP, to accumulate (Gentleman et al., 1993; Sherriff et al., 1994). This process takes time, so β-APP positivity can be used to establish a minimal survival time (Oehmichen et al., 1998; Geddes et al., 2000). Our data suggest that the mean axonal diameter might also be useful for timing a traumatic incident, since there is an approximate doubling in mean diameter from 2 to 4 μm over the first 24 h (Fig. 6). The mean axon diameter in the corpus callosum and the increase in diameter with survival time found in our study of children appear to be consistent with the adult sample we examined and also to the results described in a larger, predominantly adult, sample studied by Wilkinson et al. (1998). However, a complicating factor in the use of diameter for timing of death is the issue of concomitant hypoxia/ischemia. The four cases here in which brain death occurred prior to cessation of life support, indicate that mean axonal diameter correlated better with brain survival time than actual cessation of circulation. This suggests that axonal transport and β-APP accumulation had slowed or stopped around the time of clinical brain death, therefore preventing further axonal swelling.

Possibility for Therapeutic Intervention

The progression in both the size of damaged axons and the distribution of injury raises the question of whether the pathogenesis of axonal injury is reversible. Based on the relationship between the size of axons and survival time, Wilkinson et al. (1999) proposed three models of injury. The first is that irreversible axonal swelling may reach a plateau at around 80 h post injury, and this is supported by our data. The other models allow that lesser head injury may produce axonal swelling which will reverse after reaching a peak and that there may be a second wave of swelling some time after the initial insult as a result of secondary events such as ischemia.

Our data on the spread of injury in these pediatric cases also show an early rapid phase lasting some 10–20 h, then a slower progression. It is likely that there is also a differential progression of axonal damage in different fibre tracts since cases with less than 1 h survival did not show axonal injury in the common sites such as the corpus callosum, the parasagittal white matter or the brain stem. Experimental traumatic brain injury in animal models has shown a differing temporal course in different areas of the brain (Bramlett et al., 1997). A temporal progression from reactive change in axons at 3–6 h to fully mature, swollen axons at 24 h has been reported for rats (Povlishock and Jenkins, 1995a). The progression of axonal injury is now known to involve a complex sequence of structural and chemical changes which include disruption of the cytoskeleton, increases in intracellular calcium, and which eventually lead to a final irreversible disconnection of the axon (Povlishock and Chrisman, 1995b). While there is no accepted pharmacological intervention in the treatment of traumatic brain injury, there are a number of recent experimental studies targeting the early stages of the axonal injury cascade with a view to attenuating the damage before it becomes irreversible. Some of the newer concepts for animal studies include hypothermia (Koizumi and Povlishock, 1998), Cyclosporin A (Buki et al., 1999), magnesium (Vink et al., 2001), and Ca^{2+} channel blockers (Wolf et al., 2001). While clinical trials to date have been disappointing (Povlishock, 2000), understanding of the basic mechanisms of axonal injury can only serve as a better guide for future directions.

Our study has demonstrated that, following traumatic brain injury in children, axons begin an injury cascade within an hour with a rapid increase in the extent and distribution over the first 24 h. Axon damage is then more gradual until about 80 h when injury is distributed throughout most of the brain and axon swelling is maximal. While this is consistent with what has been reported for adults, it clearly indicates an early window of opportunity for targeted treatment when therapeutics become available.

ACKNOWLEDGMENTS

This study was supported by funding from an ARC Collaborative grant to the School of Anatomy, UNSW and the Roads and Traffic Authority, NSW. We would like to thank the Department of Forensic Medicine, Sydney Central Area Health Service, NSW and the Institute of Medical and Veterinary Science, South Australia, for their invaluable contribution to this study, and also Adam Mark and Liz Waight for their advice and technical expertise.

REFERENCES

ABOITIZ, F., SCHEIBEL, A.B., FISHER, R.S., et al. (1992). Fiber composition of the human corpus callosum. Brain Res **598,** 143–153.

ABOU-HAMDEN, A., BLUMBERGS, P.C., SCOTT, G., et al. (1997). Axonal injury in falls. J. Neurotrauma **14,** 699–713.

ADAMS, J.H., GRAHAM, D.I., MURRAY, L.S., et al. (1982). Diffuse axonal injury due to nonmissile head injury in humans: an analysis of 45 cases. Ann. Neurol. 12, 557–563.

ADAMS, J.H., DOYLE, D., GRAHAM, D.I., et al. (1986). Gliding contusions in nonmissile head injury in humans. Arch. Pathol. Lab. Med. **110,** 485–488.

ADAMS, J.H., DOYLE, D., FORD, I., et al. (1989). Diffuse axonal injury in head injury: definition, diagnosis and grading. Histopathology **15,** 49–59.

ADAMS, J.H., GRAHAM, D.I., GENNARELLI, T.A., et al. (1991). Diffuse axonal injury in non-missile head injury. J. Neurol. Neurosurg. Psychiatry **54,** 481–483.

BRAMLETT, H.M., KRAYDIEH, S., GREEM, E., et al. (1997). Temporal and regional patterns of axonal damage following traumatic brain injury: a beta-amyloid precursor protein immunocytochemical study in rats. J. Neuropathol. Exp. Neurol. **56,** 1132–1141.

BLUMBERGS, P.C., JONES, N.R., and NORTH J.B. (1989). Diffuse axonal injury in head trauma. J. Neurol. Neurosurg. Psychiatry, **52,** 838–841.

BLUMBERGS, P.C., SCOTT, G., MANAVIS, J., et al. (1995). Topography of axonal injury as defined by amyloid precursor protein and the sector scoring method in mild and severe closed head injury. J. Neurotrauma **12,** 565–572.

BLUMBERGS, P.C (1998). Changing concepts of diffuse axonal injury J. Clin. Neurosci. **5,** 123–124.

BRODY, B., KINNEY, H.C., KLOMAN, A.S., et al. (1987). Sequence of central nervous system myelination in human infancy. I. An autopsy study of myelination J. Neuropathol. Exp. Neurol. **46,** 283–301.

BUKI, A., OKONKWO, D.O., and POVLISHOCK, J.T. (1999). Postinjury cyclosporin A administration limits axonal damage and disconnection in traumatic brain injury. J. Neurotrauma **16,** 511–521.

FINNIE, J., LEWIS, S., MANAVIS, J., et al. (1999). Traumatic axonal injury in lambs: a model for paediatric axonal damage. J. Clin. Neurosci. **6,** 38–42

FITZPATRICK, M.O., MAXWELL, W.L., and GRAHAM, D.I. (1998). The role of the axolemma in the initiation of traumatically induced axonal injury J. Neurol. Neurosurg. Psychiatry **64,** 285–287.

GEDDES, J.F., WHITWELL, H.L., and GRAHAM, D.I. (2000). Traumatic axonal injury: practical issues for the diagnosis in medicolegal cases. Neuropathol. Appl. Neurobiol. **56,** 105–116.

GEDDES, J.F., HACKSHAW, A.K. VOWLES, C.D., et al. (2001). Neuropathology of inflicted head injury in children. I. Patterns of brain damage. Brain **124,** 1290–1298.

GENNARELLI, T.A., THIBAULT, L.E., ADAMS, J.H., et al. (1982). Diffuse axonal injury and traumatic coma in the primate. Ann. Neurol. **12,** 564–574.

GENTLEMAN, S.M., NASH, M.J., SWEETING, C.J., et al. (1993). β-Amyloid precursor protein (β-APP) as a marker for axonal injury after head injury. Neurosci. Lett. **160,** 139–144.

GENTRY, L.R., and GODERSKY, J.C. (1988). Trauma to the corpus callosum: MR features. Am. J. Neuroradiol. **9,** 1129–1138.

GORRIE, C., DUFLOU, J., BROWN, J., et al. (1999). Fatal head injury in children: a new approach to scoring axonal and vascular damage. Childs Nerv. Syst. **15,** 322–327.

GORRIE, C., DUFLOU, J., BROWN, J., et al. (2001). Extent and distribution of vascular brain injury in pediatric road fatalities. J. Neurotrauma **18,** 849–860.

GRAHAM, D.I., FORD, I., ADAMS, J.H., et al. (1989). Fatal head injury in children. J. Clin. Pathol. **42,** 18–22.

GRAHAM, D.I., CLARK, J.C., ADAMS, J.H., et al. (1992). Diffuse axonal injury caused by assault. J. Clin. Pathol. **45,** 840–841.

GRAHAM, D.I., McINTOSH, T.K., MAXWELL, W.L., et al. (2000). Recent advances in neurotrauma. J. Neuropathol. Exp. Neurol. **59,** 641–651.

GULTEKIN, S.H., and SMITH, T.W. (1984). Diffuse axonal injury in craniocerebral trauma. A comparative histological and immunohistochemical study. Arch. Pathol. Lab. Med. **118,** 168–171.

KOIZUMI, H., and POVLISHOCK, J.T. (1998). Posttraumatic hyperthermia in the treatment of axonal damage in an animal model of traumatic axonal injury. J. Neurosurg. **89,** 303–309

KOO, E.H., SISODA, S.S., ARCHER, D.R., et al. (1990). Precursor of amyloid protein in Alzheimer's disease undergoes fast anterograde axonal transport, Proc. Natl. Acad. Sci. U.S.A. **87,** 1561–1565.

KOSZYCA, B., BLUMBERGS, P.C., MANAVIS, J., et al. (1998). Widespread injury in gunshot wounds to the head using amyloid precursor protein as a marker. J. Neurotrauma **15,** 675–683.

LECLERCQ, P.D., McKENSIE, J.E., GRAHAM, D.I., et al. (2001). Axonal injury is accentuated in the caudal corpus callosum of head injured patients. J. Neurotrauma **18,** 1–9.

LEWIS, S.B., FINNIE, J.W., BLUMBERGS, P.C., et al. (1996). A head impact model of early axonal injury in the sheep. J. Neurotrauma **13,** 505–514.

MAXWELL, W.L., WATT, C., GRAHAM, D.I., et al. (1993). Ultrastructural evidence of axonal shearing as a result of lateral acceleration of the head in non-human primates. Acta Neuropathol. **86,** 136–144.

MAXWELL, W.L., POVLISHOCK, J.T., and GRAHAM, D.I. (1997). A mechanistic approach to nondisruptive axonal injury: a review. J. Neurotrauma **14,** 419–440.

McKENZIE, K.J., McLELLAN, D.R., GENTLEMAN, S.M., et al. (1996). Is beta-APP a marker of axonal damage in short-surviving head injury. Acta Neuropathol. **92,** 608–613.

MEANEY, D., SMITH, D., SHREIBER, D., et al. (1995). Biomechanical analysis of experimental diffuse axonal injury. J. Neurotrauma **12,** 689–694.

MENDELSOHN, D.B., LEVIN, H.S., and BRUCE, D. (1992). Corpus callosum lesions after closed head injury in children: MRI, clinical features and outcome. Neuroradiology **34,** 384–388.

NISHIMOTO, T., and MURAKAMI, S. (1998). Relation between diffuse axonal injury and internal head structures on blunt impact. J. Biomed. Eng. **120,** 140–147.

OEHMICHEN, M., MEISSNER, C., SCHMIDT, V., et al. (1998). Axonal injury—a diagnostic tool in forensic neuropathology—a review. Forensic Sci. Int. **95,** 67–83.

POLITIS, N.J., and INGOGLIA, N.A. (1979). Axonal transport of taurine along neonatal and young adult rat optic axons. Brain Res. **166,** 221–231.

POVLISHOCK, J.T. (1992). Traumatically induced axonal injury: pathogenesis and pathobiological implications. Brain Pathol. **2,** 1–12.

POVLISHOCK, J.T., and JENKINS, L.W. (1995a). Are the pathobiological changes evoked by traumatic brain injury immediate and irreversible. Brain Pathol. **5,** 415–426.

POVLISHOCK, J.T., and CHRISMAN, C.W. (1995b). The pathobiology of traumatically induced axonal injury in animals and humans: a review of current thoughts. J. Neurotrauma **12,** 555–564.

POVLISHOCK, J.T. (2000). Pathophysiology of neural injury: therapeutic opportunities and challenges. Clin. Neurosurg. **46,** 113–126.

RUSS, J.C. (1994). *The Image Processing Handbook*, 2nd ed. CRC Press: Boca Raton, FL.

SHERRIFF, F.E., BRIDGES, L.R., and GENLEMAN, S.M. (1994). Markers of axonal injury in post mortem human brain. Acta Neuropathol. **88,** 433–439.

SLAZINSKI, T., and JOHNSON, M.C. (1994). Severe diffuse axonal injury in adults and children J. Neurosci. Nurs. **26,** 151–154.

SMITH, D., XIAO-HAN, C., BAI-NAN, X., et al. (1997). Characterization of diffuse axonal pathology and selective hippocampal damage following inertial brain trauma in the pig. J. Neuropathol. Exp. Neurol. **56,** 822–834.

TEMPLETON, J.M. (1993). Mechanism of injury: biomechanics, in: *Pediatric Trauma.* M.R. Eichelberger (ed), Mosby–Year Book: St Louis, MO, pps. 20–38.

VIANCOUR, T.A., and KREITER, N.A. (1993). Vesicular fast axonal transport rates in young and old rat axons. Brain Res. **628,** 209–217.

VINK, R., NIMMO, J., and CERNAK, I. (2001). An overview of new and novel pharmacotherapies for use in traumatic brain injury. Clin. Exp. Phamacol Physiol. **28,** 919–921.

WAXMAN, S.G., BLACK, J.A., RANSOM, B.R., et al. (1993). Protection of the axonal cytoskeleton in anoxic optic nerve by decreased extracellular calcium. Brain Res. **614,** 137–145.

WILKINSON, A.E., BRIDGES, L.R., and SIVALOGANATHAN, S. (1999). Correlation of survival time with size of axonal swellings in diffuse axonal injury. Acta Pathol. **98,** 197–202.

WOLF, J. A., STYS, P.K., LUSARDI, T., et al. (2001). Traumatic axonal injury induces calcium influx modulated by tetrodotoxin-sensitive sodium channels. J. Neurosci. 21, 1923–1930.

Address reprint requests to:
Catherine Gorrie
Neural Injury Research Unit
Department of Anatomy
School of Biomedical Sciences
Wallace Wurth Blg.
University of New South Wales
UNSW Sydney 2052, Australia

E-mail: c.gorrie@unsw.edu.au